

Control of spiking regularity in a noisy complex neural network

Qianshu Li^{1,2,*} and Yang Gao¹

¹*The Institute for Chemical Physics, Beijing Institute of Technology, Beijing, China, 100081*

²*School of Chemistry and Environment, South China Normal University, Guangzhou, China, 510006*

(Received 24 July 2007; revised manuscript received 4 December 2007; published 19 March 2008)

The effects of spatiotemporally correlated noise on the regularity of spiking oscillations are studied in a network composed of Fitz-Hugh-Nagumo neurons. The spiking regularity of the neural network becomes the best at a moderate noise intensity, indicating the occurrence of coherence resonance (CR). The CR in a Watts-Strogatz small-world network is further improved by adding a small fraction of long-range connections. Given a set of temporal correlation constant τ and spatial correlation length λ of the noise, there exists an optimal network topology randomness, at which the spiking oscillations show the best regularity. The optimal randomness of the network topology at different τ and λ varies in a narrow range. Changing λ does not affect the optimal τ for achieving the most regular spike train, whereas varying τ , the best spiking regularity emerges at different optimal λ .

DOI: [10.1103/PhysRevE.77.036117](https://doi.org/10.1103/PhysRevE.77.036117)

PACS number(s): 84.35.+i, 82.40.Bj, 89.75.-k

I. INTRODUCTION

In nature, many systems are exposed to inherent noise, or are subjected to the action of external noise. In nonlinear systems, noise in some cases can play constructive roles. Perhaps the best known of these are stochastic resonance (SR), in which the response of a system to a weak signal is enhanced most at an optimal noise strength [1], and coherence resonance (CR), in which the regularization of the system response is maximized at an optimal noise intensity without an external drive [2]. In neuroscience, SR and CR have been studied extensively in experiments and in theories [3–9]. For instance, the sensory mechanoreceptors of crayfish can detect a very weak water movement of about 10 nm by means of SR [3]. Experimental evidence of CR has been reported in the coherence between spinal and cortical neurons in the somatosensory system of the anaesthetized cat [9]. Recently, SR or CR in coupled systems has also drawn great interests. Coupling can effectively enhance the phenomenon of SR or CR in the system of coupled units beyond that of the individual unit. Such behaviors are called array-enhanced stochastic resonance (AESR) [10] or array-enhanced coherence resonance (AECR) [11]. In neuronal systems, coupling between neurons can improve their signal-processing capabilities through AESR or AECR [12–14].

In coupled systems, two ingredients may have significant effects on the systems' collective behaviors: (i) noise correlation, including temporal correlation and spatial correlation, and (ii) the topology of connecting structure. In most of the previous investigations, fluctuations are typically accounted for by white noise, namely, temporally independent noise. However, for most systems, white noise is not a good approximation of the actual fluctuations present in the system which are frequently colored noise (temporally correlated noise). Experimental results [15,16] have demonstrated that colored noise, rather than white noise, provides the best

model for the background input. Spatially correlated noise also attracted increasing attention [17,18]. It has been suggested that neurons receive synaptic inputs from a large number of other neurons, and these inputs may be highly correlated [19]. Thus the spatial correlation in input noise must be taken into account in some cases.

As to the topological structure of a network, a prominent type is “small-world” topological structure introduced by Watts and Strogatz [20,21] among various network topologies. Many real-world networks exhibit geometrical properties of small-world network [22]. For example, neuron connectivity in the cortex and other brain regions is mainly local, with relatively sparse long-distance projections, suggesting the small-world topological structure. Earlier small-world network investigations mostly focused on the topological properties of the networks and various mechanisms to determine the topology. Recent research is engaged in understanding how the network topology influences the system's dynamical behaviors [23–26]. For example, it has been shown that small-world connections can enhance the probability of spiral wave's formation in excitable media [25]. Different avalanche behaviors have been found for different density of long-range connections in the small-world neural networks [26]. These studies demonstrate that small-world topological structure plays a crucial role for systems' dynamics.

The effects of the randomness of the network topology and the noise spatial correlation on the coherence factor have been investigated in Ref. [27]. In our work, the effect of the noise temporal correlation on coherence resonance is further investigated in a network of Fitz-Hugh-Nagumo (FHN) excitable cells. We mainly explore the general influences of the network topological structure and the noise spatiotemporal correlation on the dynamical behaviors of the system. It is found that compared to that in a regular or in a completely random network, CR can be enhanced in a small-world network. When changing the temporal correlation constant τ and spatial correlation length λ of the noise, the optimal randomness of the network topology for the best spiking regularity varies slightly. For different λ , the optimal τ of the

*Corresponding author. FAX: +86-10-6891-2665.
qqli@bit.edu.cn

noise keeps unchanged for the best spiking regularity, while the optimal λ increases with τ increasing.

II. MODEL AND METHODS

The model used here consists of N ($N=100$) FHN neurons in which a small-world network topology is constructed as follows. First, a regular lattice is considered, in which each neuron connects to its K ($K=4$) nearest neighbors. Next, each local link is visited once and, with the rewiring probability p , removed and reconnected to a randomly chosen neuron. It should be noted that a lot of network realizations exist for a given p . The rewiring parameter p takes different values between 0 and 1 and controls the topology of the network: if $p=0$, only local connections are present, and conversely if $p=1$, any two neurons in the network can be connected with the same probability (global connectivity). The FHN model investigated in this work is simplified from the Hodgkin-Huxley (HH) model and its dynamics provides a simple representation of the firing dynamics of sensory neurons. This model has been utilized to investigate various dynamical processes, such as spiral wave [28], synchronization [29], stochastic resonance [30,31], and coherence resonance [32,33]. The latter has especially garnered more interest in literature. The dynamics of each FHN neuron is described by the following equations:

$$\varepsilon \frac{dx_i}{dt} = x_i - \frac{x_i^3}{3} - y_i + g_{ij}(x_j - x_i) + \xi_i(t), \quad (1)$$

$$\frac{dy_i}{dt} = x_i + a_i, \quad (2)$$

where $x_i(t)$ is a fast variable representing the membrane voltage of i th neuron, and $y_i(t)$ is a slow recovery variable. The time scale separation ε is set to 0.01 and the bifurcation parameter a_i is assumed the same for every neuron and is set to 1.02 so that the dynamics has only a stable focus but is close to the supercritical Hopf bifurcation at $a_i=1$. g_{ij} is the coupling parameter between the two neurons i and j , and its value is determined by the coupling pattern of the system. If these two neurons are coupled to each other, g_{ij} is a determinate value g , otherwise, $g_{ij}=0$.

The spatiotemporally correlated noise ξ_i is generated with the method in Ref. [27] by summing N Gaussian colored noise with correlation function m_k ,

$$\xi_i = \frac{1}{\sqrt{\sum_{k \in \Lambda} m_k^2}} \sum_{k \in \Lambda} C_{i+k} m_k, \quad (3)$$

$$\Lambda = \{-4\lambda, \dots, -2, -1, 0, 1, 2, \dots, 4\lambda\}, \quad (4)$$

where C_i is Gaussian colored noise with zero mean and correlation given by $\langle C_i(t_1)C_i(t_2) \rangle = (D/\tau)\exp(-\frac{|t_1-t_2|}{\tau})$. This colored noise is produced by the Ornstein-Uhlenbeck (OU) stochastic process and can be depicted by

$$\tau \frac{dC_i}{dt} = -C_i + \zeta_i(t), \quad (5)$$

in which $\zeta_i(t)$ is Gaussian white noise with $\langle \zeta_i(t) \rangle = 0$ and $\langle \zeta_i(t)\zeta_i(t') \rangle = 2D\delta(t-t')$. D is the strength of $\zeta_i(t)$. The correlation function among neurons is defined by $m_k = \exp(-2k^2/\lambda^2)$. Thus, ξ_i is spatiotemporally correlated noise defined by $\langle \xi_i(t) \rangle = 0$ and $\langle \xi_i(t)\xi_j(t') \rangle = (D/\tau)\exp(-\frac{|i-j|^2}{\lambda^2}) \times \exp(-\frac{|t-t'|}{\tau})$. It should be noted that i and j denote the spatial positions of neurons in the network, and $|i-j|$ represents a distance along the network.

III. RESULTS AND DISCUSSION

The stochastic differential equations (1) and (2) are numerically integrated using the Euler scheme with a fixed time step of 0.002. It has been reported that in a neuron the noise-induced oscillations are rather irregular for small and large noise amplitudes, while exhibit relatively periodic activity for a moderate noise intensity [2]. Here we focus on the collective behavior of the network and measure the average activity $x(t) = (1/N)\sum_{i=1}^N x_i(t)$. The spatiotemporal evolution of all 100 neurons in the network and the corresponding collective network behaviors with different noise intensity are shown in the left and right columns of Fig. 1, respectively. As expected, behavior similar to a single neuron occurs, namely, Fig. 1(d) with moderate noise intensity showing the most regular oscillations in the right three plots. As oscillations are induced by noise in each neuron, there are very few spikes for very small noise strength. On the contrary, if the noise intensity is large, although the spike firing becomes more frequently, the regularity of the spike train is smeared by the strong noise. Consequently, for an intermediate noise intensity, the spike train is the most regular. Moreover, it can be seen from the entire network firing events on the left column of Fig. 1, that the spatial coherence between neurons is decreased with the increase of the noise intensity. As oscillations are induced by noise in each neuron, neurons subjected to different noise will display different oscillation behaviors. The stronger the noise intensity, the larger the differences of the oscillations, and as a consequence, the poorer the degree of synchronization among individual neurons.

To characterize the temporal coherence of the collective oscillations of a network quantitatively, the coherence factor of the variable x is obtained by the following formula [2]:

$$R = \frac{\sqrt{\text{Var}(T_k)}}{\langle T_k \rangle}. \quad (6)$$

Here, $T_k = t_{k+1} - t_k$, and t_k is the time of the k th pulse in the time series of x . A smaller R corresponds to a better spiking regularity. Biologically, this quantity is of importance because it is related to the timing precision of the information processing in neural systems [34]. Note that a pulse occurs when the state variable x exceeds a certain threshold value x_0 (here taken arbitrarily as $x_0=0.5$) and it turns out that the threshold value can vary in a wide range without altering the results.

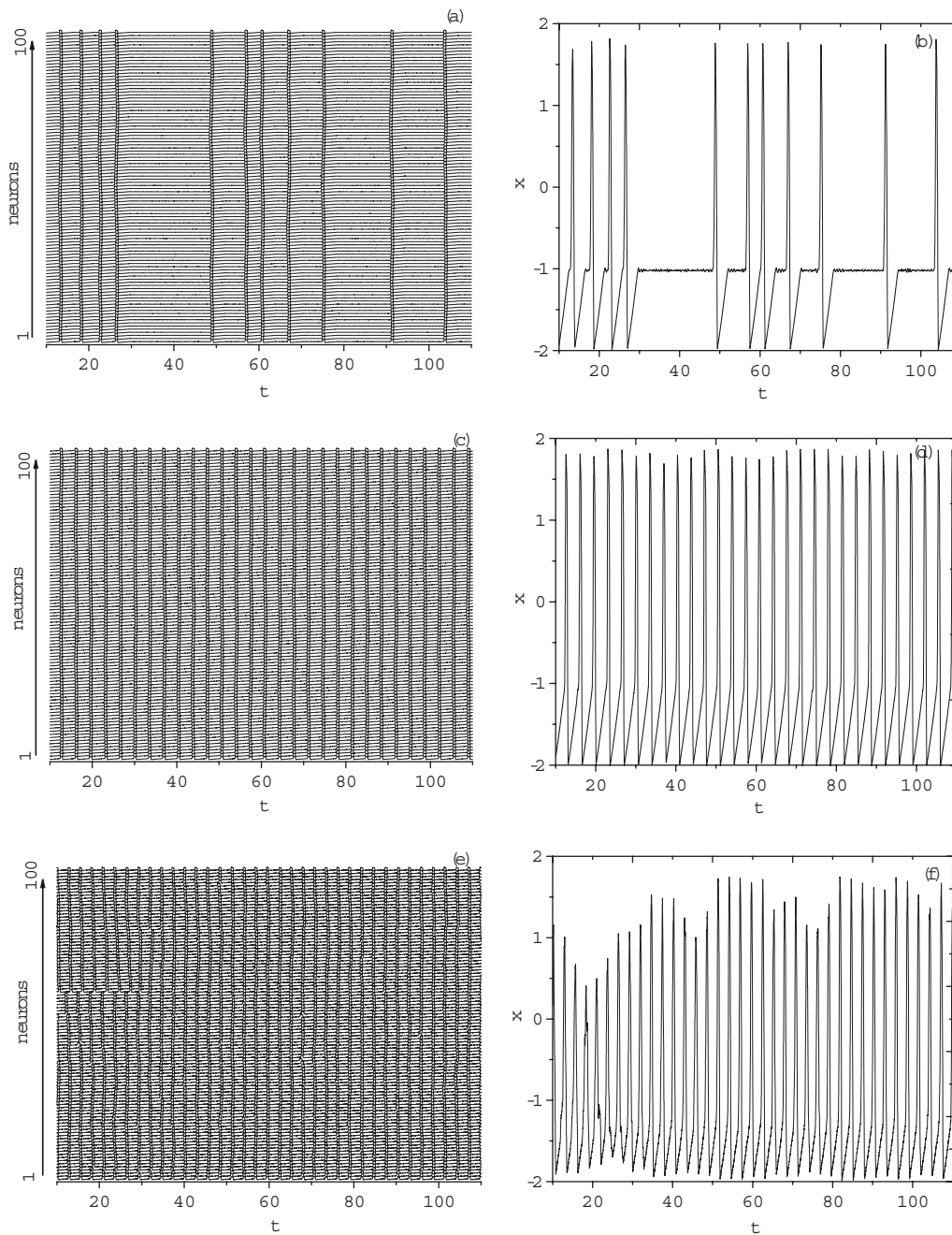


FIG. 1. The spatiotemporal evolution of all 100 neurons on the left column and the corresponding collective time series on the right column at $\varepsilon=0.01$, $a=1.02$, $g=0.05$, $p=0.05$, $\tau=0.05$, $\lambda=1$. From top to bottom $D=0.00008$, 0.00025 , and 0.0015 .

First, the influence of the coupling between units on the activation of the network is investigated. Figure 2 displays the dependence of the coherence factor R on the noise intensity D achieved at different coupling strength g . Here each R is attained by averaging over 30 network realizations for each p . It can be seen that every curve shows a typical CR characteristic, i.e., first a drop and then a rise with the increase of the noise intensity. The lowest point of each curve in Fig. 2 is called maximal coherence factor signed by R_m , and the noise intensity at R_m is called optimal noise intensity D_{opt} . When the coupling between units is weak ($g=0.01, 0.03$), the corresponding R_m is large, showing depressed temporal coherence. When the coupling becomes

strong ($g=0.05, 0.1$), the spiking regularity of the system is improved. When the coupling strength increases further such as $g=0.3$, R_m rises instead of dropping (in order to show clear variations of R at other coupling strength, the data for R at $g=0.3$ are not shown here). Comparing the curve at $g=0.05$ with that at $g=0.1$, it is found that the values of R_m are very close; however, the optimal noise intensity D_{opt} is apparently larger for the latter. Therefore, $g=0.05$ is considered as a proper coupling strength and will be adopted throughout this paper.

Figures 3(a)–3(d) depict the coherence factor R versus the noise intensity D achieved at different rewiring probability p and spatial correlation length λ of the noise. The correlation

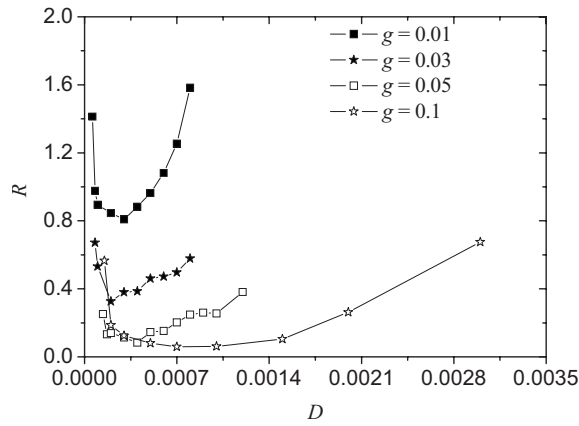


FIG. 2. The coherence factor R versus the noise intensity D at different coupling strengths. $p=0.2$, $\tau=0.2$, and $\lambda=2$.

time τ of the noise is 0.02. It can be observed that R_m is the smallest at $\lambda=0$ in each plot, which implies that the spiking regularity of the system is the best when the noise is spatially independent. This behavior can be explained based on the interplay among these neurons. In the case of spatially independent noise ($\lambda=0$), neurons with completely different

noise fire spikes independently. As λ increases, the correlation in input noise among neurons is enhanced, and more neurons are prone to rest or to fire synchronously, which improves the spatial synchronization among the behaviors of all the neurons. Inversely, the high synchronized activation of all units prevents excitation by noise, which leads to the decrease of the coherent motion [27,35]. Therefore, the value of R_m increases with the increase of λ . These results imply that large λ plays a negative role in enhancing CR, which is similar to some previous studies [13,36,37]. In addition, with the increase of λ , the position of D_{opt} moves towards smaller D . Moreover, the variation range of D_{opt} at different λ becomes narrow gradually when the rewiring probability p increases from 0 to 1, which means that the influence of λ on the dynamical behaviors of the network becomes weaker with the increase of the disorder of the network topology. For a regular network ($p=0$), large λ makes each neuron interact with the ones exposed to the spatially correlated noise. However, increasing the disorder of the network makes each neuron able to interact with distant ones exposed to an uncorrelated noise and reduces the spatial correlation of the noise.

Figures 4(a)–4(d) show how the coherence factor R changes with the noise intensity D at different rewiring probability p and temporal correlation constant τ of the noise.

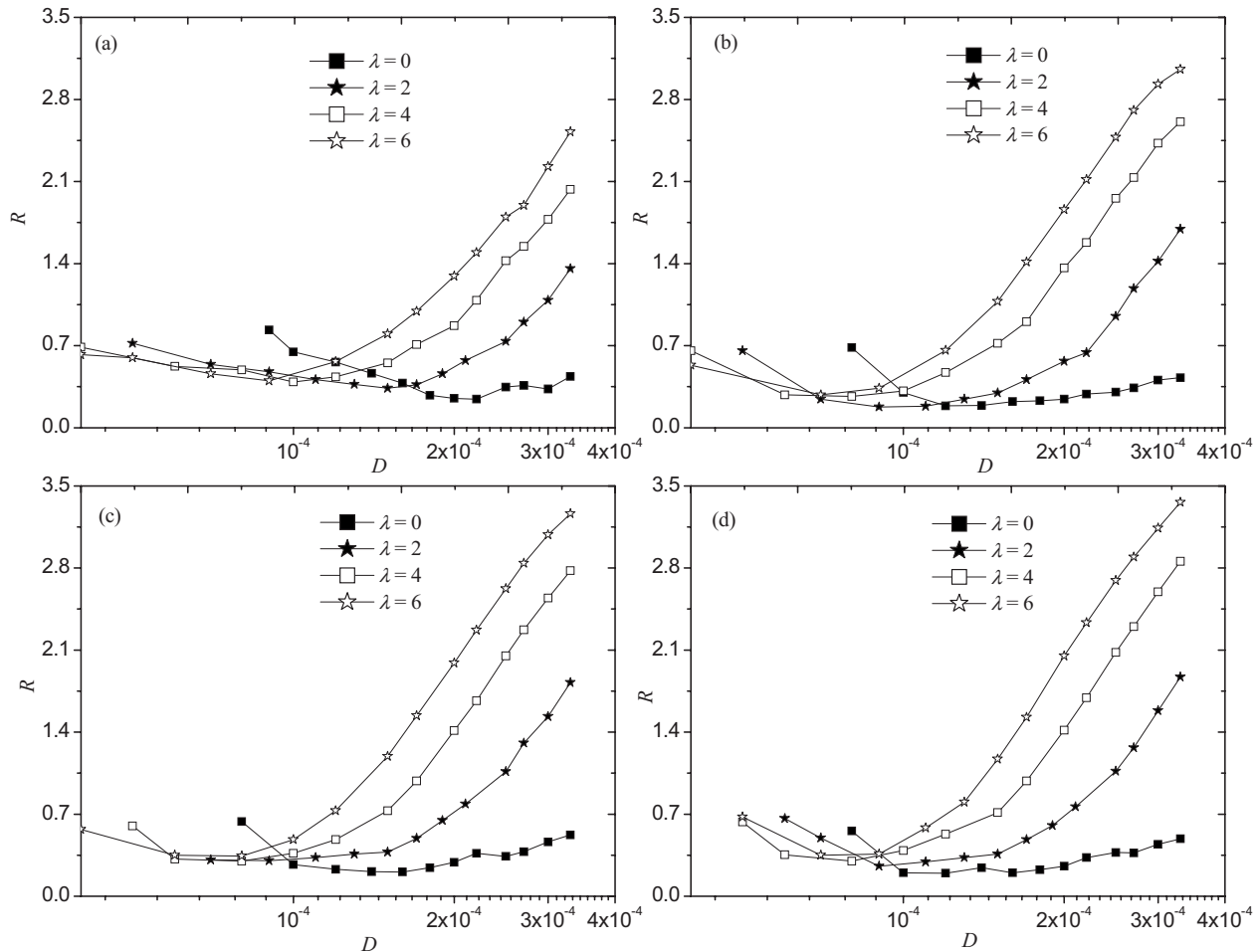


FIG. 3. The coherence factor R versus the noise intensity D at different spatial correlation lengths λ of the noise in (a) the regular network ($p=0$); (b) and (c) the small-world networks with $p=0.20$, and $p=0.50$, respectively; (d) the completely random network ($p=1$). $g=0.05$ and $\tau=0.02$.

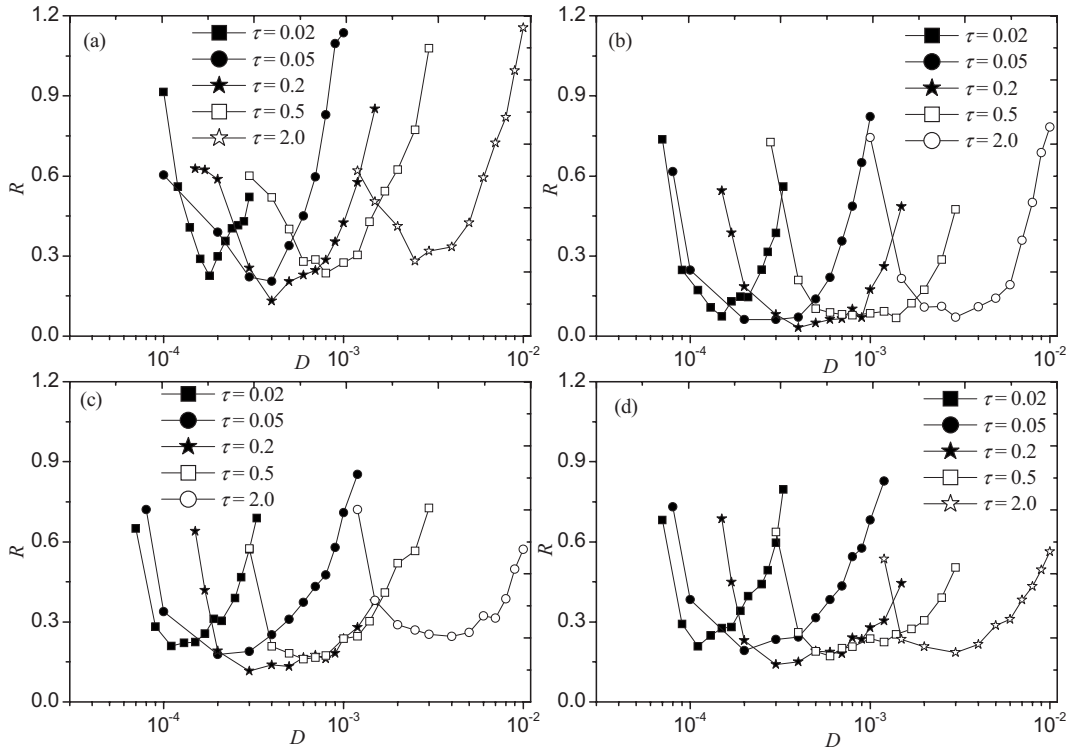


FIG. 4. The coherence factor R versus the noise intensity D at different correlation times τ of the noise in (a) the regular network ($p=0$); (b)–(d) the small-world networks with $p=0.05$, $p=0.2$, and $p=0.50$, respectively. $g=0.05$ and $\lambda=1$.

Here the spatial correlation length λ is 1. Each R_m is the smallest at $\tau=0.2$ whatever p is, therefore there exists an optimal noise correlation time $\tau=0.2$. Similar results are obtained for other λ values and the corresponding figures are omitted. As the noise correlation time increases, D_{opt} takes a larger value, that is, a stronger noise is needed to excite the neurons. When the noise spatial correlation is fixed, the spatiotemporally correlated noise is actually characterized by two parameters, the noise intensity D and the correlation time τ . The measurement of the amplitude of the noise can be characterized by $\sigma=\sqrt{D/\tau}$ [38]. It can be seen that σ varies directly proportional to D , but inversely proportional to τ . Thus, the increment of τ is equivalent to the decrease of D , vice versa. It is known that there exists an optimal noise intensity corresponding to the best spiking regularity in the network. So there definitely exists an optimal noise correlation time.

Comparing R_m values at the same τ for different values of p in Fig. 4, R_m at $p=0.05$ has the smallest value. Then, there may be an optimal rewiring probability corresponding to the best spiking regularity. R versus D at different p is plotted in Fig. 5, in which $\tau=0.05$ is taken as an example. It can be seen that CR is enhanced in a small-world network. The plot also shows that R_m at $p=0.05$ is the smallest, which further assures that $p=0.05$ is the optimal rewiring probability in this case. It is emphasized that for various τ , there still exists an optimal rewiring probability around $p=0.05$, as shown in Fig. 7. Usually, a small-world network is characterized by two important parameters: a small average path length $L(p)$ and a large clustering coefficient $C(p)$. Here, $L(p)$ is defined as the number of edges in the shortest path between two

neurons, averaged over all pairs of neurons. $C(p)$ is defined as the extent to which neurons connected to any neuron are connected to each other. It can be seen from Fig. 6 that the “small-world properties” of the network are especially apparent when p varies from 0.05 to 0.10. Therefore, the positive role of small-world topology to enhance the CR of the system is remarkable when p emerges in this range. In fact, in some previous work concerning small-world networks, it was also found that certain remarkable dynamical behavior can appear for an optimal randomness of the network topological structure. For example, an optimal level of topological randomness exists such that the system has maximum order and the spatiotemporal chaos is tamed in an array of coupled pendulum networks [39]. In the coupled Hodgkin-Huxley neurons, there are optimal random shortcuts where

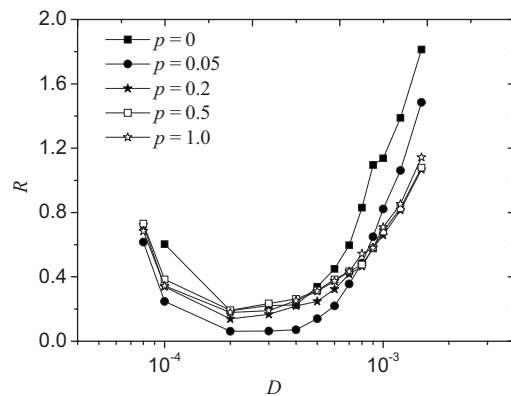


FIG. 5. The coherence factor R versus the noise intensity D at different rewiring probabilities p . $g=0.05$, $\lambda=1$, and $\tau=0.05$.

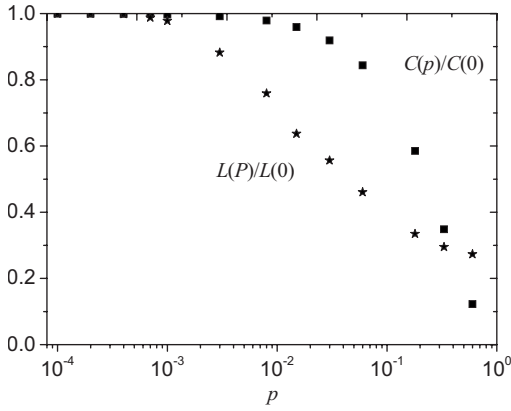


FIG. 6. Characteristic path length L , clustering coefficient C as a function of the rewiring probability p in Watts-Strogatz small-world networks with $N=100$ and $K=4$. They are normalized by each value at $p=0$.

the collective spike coherence and individual one conduct the best temporal coherence [40].

In order to explore comprehensively the influences of the three parameters p , λ , and τ on the spiking regularity of the system, the maximal coherence factor R_m as a function of the network topology randomness p at different values of λ is depicted in the plots of Fig. 7. Figure 7(a) denotes the case taking a small noise correlation time ($\tau=0.02$), while Fig. 7(b) is an example using an intermediate noise temporal correlation constant ($\tau=0.2$), and Fig. 7(c) is the case with a large noise correlation time ($\tau=2.0$). As discussed above, R_m is the smallest at $\tau=0.2$ when all other parameters are fixed. Moreover, it can be observed that the optimal rewiring probability p in each curve ranges from 0.05 to 0.1 in all three plots, which agrees well with the network topological characteristics shown in Fig. 6.

Another prominent behavior shown in Fig. 7 is that as τ increases, λ corresponding to the minima of R_m also increases. When $\tau=0.02$, the curve lies in the lowest position if $\lambda=0$, which has been discussed in Fig. 3. When τ increases to 0.2, R_m takes the smallest value at each p if $\lambda=1$. When $\tau=2.0$, the spatial correlation length of the noise corresponding to the smallest R_m at each p is 2. These results suggest that large λ is helpful for enhancing the regularity of the spike train of the network when the correlation time τ becomes larger. This fact can be understood from two points of view: (i) By looking at the expression for the noise correlation function $\langle \xi_i(t)\xi_j(t') \rangle = (D/\tau)\exp(-\frac{|i-j|^2}{\lambda^2})\exp(-\frac{|t-t'|}{\tau})$, it can be found that for two consecutive neurons in the network, the noise intensity varies directly proportional to λ , but inversely proportional to τ . Therefore, when the temporal correlation of the noise increases, the spatial correlation of the noise should also increase, thus producing a ‘‘compensation’’ effect to maintain the proper noise intensity needed for coherence. (ii) As the correlation time of the noise increases, the deterministic component of the noise term is enhanced, while the proportion of the stochastic component reduces. In the long correlation time limit $\tau \rightarrow \infty$, the deterministic behavior is recovered [41]. In this case there are two ways to strengthen the stochastic part: one is to increase the noise

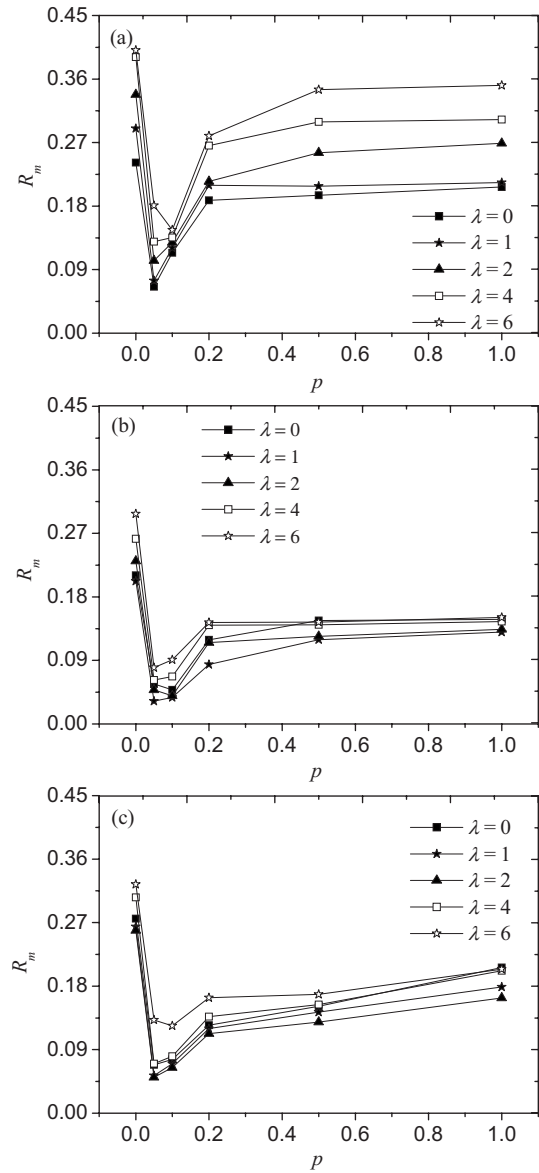


FIG. 7. The maximal coherence factor R_m versus the rewiring probability p at different spatial correlation length λ of the noise. (a) $\tau=0.02$; (b) $\tau=0.2$; (c) $\tau=2.0$. $g=0.05$.

intensity, and the other is to enhance the spatial correlation length of the noise so that the stochastic part of the noise term in each neuron can reinforce each other. Obviously, increasing the noise intensity alone can not be satisfied. The optimal noise D_{opt} against the spatial correlation length λ of the noise is plotted in Fig. 8. Horizontally, it can be seen that D_{opt} tends toward smaller value as λ increases. Vertically, it can be observed that D_{opt} moves toward larger value with the increase of the correlation time τ of the noise. Furthermore, the effect of τ on D_{opt} is evidently larger than that of λ , resulting in the fact that the coherence curves are closer to each other near quite flat optimal intervals in Fig. 3 than those in Fig. 4. Comparison of Figs. 7 and 8 illustrates that when τ increases, properly enhancing λ can induce more regular spiking with smaller D_{opt} value. Usually, a large spatial correlation length is considered to degrade coherence resonance of a system [13,36,37]; however, in the case of

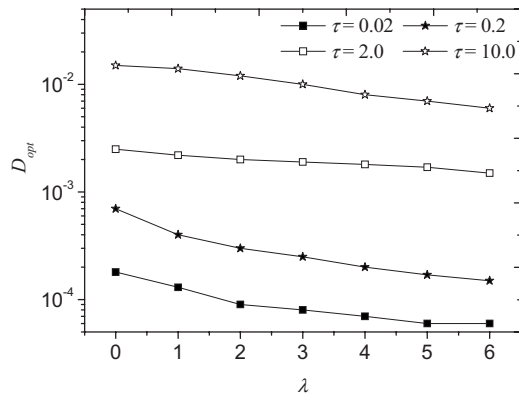


FIG. 8. The optimal noise intensity D_{opt} against the spatial correlation λ of the noise at different correlation time τ of the noise. $g=0.05$, and $p=0.10$.

large temporal correlation it is found that improved coherence resonance can be obtained by increasing the spatial correlation length of the noise.

As mentioned above, the influence of each control parameter, such as the coupling strength, the rewiring probability, and the spatiotemporally correlated levels of the noise etc., on the dynamical behaviors of the network are characterized mainly by two factors, the maximal coherence factor R_m and the optimal noise intensity D_{opt} . Within the whole selected range of these control parameters, the effect of the noise temporal correlation τ on D_{opt} is stronger than those of other parameters, while it is difficult to distinguish which parameter R_m is more sensitive to. It is known that only parameters λ and τ have a direct relationship with D [see the noise correlation expression $\langle \xi_i(t)\xi_j(t') \rangle = (D/\tau)\exp(-\frac{|i-j|^2}{\lambda^2}) \times \exp(-\frac{|t-t'|}{\tau})$]. Moreover, Fig. 8 illustrates that the variation of τ has a larger impact on D than on λ . So, among all the discussed parameters, the correlation time of the noise has the strongest influence on the D_{opt} . Anyway, these individual parameters constitute an integrated system, and the spiking regularity can be optimized through the interplay of these parameters.

IV. SUMMARY

This paper investigates the effects of the network topology and the spatiotemporally correlated noise on the spiking

regularity in networks composed of Fitz-Hugh-Nagumo neurons with the emphasis on the networks with Watts-Strogatz small-world topological structure. The constructive role of noise is discussed and coherence resonance phenomenon is observed in the networks. It is found that coherence resonance can be improved by merely adding a small fraction of long-range connections in the regular network. In addition, there exists a narrow network topology randomness range that covers the optimal randomness of the network topological structure at different spatiotemporal correlation levels of the noise. Moreover, when the spatial correlation length λ of the noise increases, the spiking of the system is the most regular at the same temporal correlation constant τ of the noise regardless the network topological structure. When the correlation time τ increases, the best spiking regularity of the system emerges at a larger spatial correlation length λ .

It is known that collective oscillations of a group of neurons are common in the brain and are thought to play a critical role in various physiological schemes. Meanwhile, the brain is the most complex and fascinating processor, and the neuron activity in the brain is subjected to many factors. Our results indicate that the collective spiking regularity of the neural network can be modulated by controlling the network topological structure and the level of correlation of the noise. These results discussed above shall provide further insights into the detailed dynamics of complex phenomena taking place in some real neuronal circuits or neuron systems whose connection structures are similar to those discussed in this paper. The role of long-range connections have been explored in detail in topological analyses of neural connectivity [42,43]. However, to our knowledge, there are few investigations about the combined influences of network topological structures, noise spatiotemporal correlation, and noise strength on the dynamical behaviors in a system. We hope that the interplay of these parameters can result in some new phenomena.

ACKNOWLEDGMENTS

This work was supported by the National Natural Science Foundation of China (Grant No. 20433050) and the 111 project (B07012) in China.

[1] R. Benzi, A. Sutera, and A. Vulpiani, *J. Phys. A* **14**, L453 (1981).
 [2] A. S. Pikovsky and J. Kurths, *Phys. Rev. Lett.* **78**, 775 (1997).
 [3] S. M. Bezrukov and I. Vodyanoy, *Nature (London)* **378**, 362 (1995).
 [4] J. K. Douglass, L. Wilkens, E. Pantazelou, and F. Moss, *Nature (London)* **365**, 337 (1993).
 [5] J. E. Levin and J. P. Miller, *Nature (London)* **380**, 165 (1996).
 [6] J. J. Collins, T. T. Imhoff, and P. Grigg, *Nature (London)* **383**, 770 (1996).
 [7] Y. Kashimori, H. Funakubo, and T. Kambara, *Biophys. J.* **75**,

1700 (1998).
 [8] E. Simonotto, M. Riani, C. Seife, M. Roberts, J. Twitty, and F. Moss, *Phys. Rev. Lett.* **78**, 1186 (1997).
 [9] E. Manjarrez, J. G. Rojas-Piloni, I. Méndez, L. Martínez, D. Vélez, D. Vázquez, and A. Flores, *Neurosci. Lett.* **326**, 93 (2002).
 [10] J. F. Lindner, B. K. Meadows, W. L. Ditto, M. E. Inchiosa, and A. R. Bulsara, *Phys. Rev. Lett.* **75**, 3 (1995).
 [11] B. Hu and C. S. Zhou, *Phys. Rev. E* **61**, R1001 (2000).
 [12] S. K. Han, T. G. Yim, D. E. Postnov, and O. V. Sosnovtseva, *Phys. Rev. Lett.* **83**, 1771 (1999).

- [13] W. Wang and Z. D. Wang, Phys. Rev. E **55**, 7379 (1997).
- [14] C. S. Zhou, J. Kurths, and B. Hu, Phys. Rev. Lett. **87**, 098101 (2001).
- [15] A. Destexhe, M. Rudolph, J.-M. Fellous, and T. J. Sejnowski, Neuroscience **107**, 13 (2001).
- [16] A. Destexhe, M. Rudolph, and D. Paré, Nat. Rev. Neurosci. **4**, 739 (2003).
- [17] C. Hauptmann, F. Kaiser, and C. Eichwald, Int. J. Bifurcation Chaos Appl. Sci. Eng. **9**, 1159 (1999).
- [18] S. Alonso, F. Sagués, and J. M. Sancho, Phys. Rev. E **65**, 066107 (2002).
- [19] K. H. Britten, M. N. Shadlen, W. T. Newsome, and J. A. Movshon, J. Neurosci. **12**, 4745 (1992).
- [20] D. J. Watts, *Small Worlds* (Princeton University Press, Princeton, 1999).
- [21] D. J. Watts and S. H. Strogatz, Nature (London) **393**, 440 (1998).
- [22] R. Albert and A.-L. Barabási, Rev. Mod. Phys. **74**, 47 (2002).
- [23] A. R. Atilgan, P. Akan, and C. Baysal, Biophys. J. **86**, 85 (2004).
- [24] F. Jasch and A. Blumen, J. Chem. Phys. **117**, 2474 (2002).
- [25] D. He, G. Hu, M. Zhan, W. Ren, and Z. Gao, Phys. Rev. E **65**, 055204(R) (2002).
- [26] M. Lin and T. L. Chen, Phys. Rev. E **71**, 016133 (2005).
- [27] O. Kwon, H. H. Jo, and H. T. Moon, Phys. Rev. E **72**, 066121 (2005).
- [28] X. Wang, Y. Lu, M. Jiang, and Q. Ouyang, Phys. Rev. E **69**, 056223 (2004).
- [29] H. Hasegawa, Phys. Rev. E **70**, 066107 (2004).
- [30] D. Nozaki, J. J. Collins, and Y. Yamamoto, Phys. Rev. E **60**, 4637 (1999).
- [31] D. Nozaki and Y. Yamamoto, Phys. Lett. A **243**, 281 (1998).
- [32] B. Lindner and L. Schimansky-Geier, Phys. Rev. E **61**, 6103 (2000).
- [33] P. Gong, J. Xu, and S. Hu, Chaos, Solitons Fractals **13**, 885 (2002).
- [34] X. Pei, L. Wilkens, and F. Moss, Phys. Rev. Lett. **77**, 4679 (1996).
- [35] S. Wang, F. Liu, W. Wang, and Y. Yu, Phys. Rev. E **69**, 011909 (2004).
- [36] F. Liu, B. Hu, and W. Wang, Phys. Rev. E **63**, 031907 (2001).
- [37] B. Lindner, B. Doiron, and A. Longtin, Phys. Rev. E **72**, 061919 (2005).
- [38] J. M. Buldú, J. Garcia-Ojalvo, C. R. Mirasso, M. C. Torrent, and J. M. Sancho, Phys. Rev. E **64**, 051109 (2001).
- [39] M. Wang, Z. Hou, and H. Xin, ChemPhysChem **7**, 579 (2006).
- [40] Y. Gong, M. Wang, Z. Hou, and H. Xin, ChemPhysChem **6**, 1042 (2005).
- [41] J. M. Sancho and M. San Miguel, *Noise in Nonlinear Dynamical Systems* (Cambridge University Press, Cambridge, 1989).
- [42] G. Buzsáki, C. Geisler, D. A. Henze, and X. J. Wang, Trends Neurosci. **27**, 186 (2004).
- [43] M. Kaiser and C. C. Hilgetag, Neurocomputing **58-60**, 297 (2004).